

Spectrum Cartography using Adaptive Radial Basis Functions: Experimental Validation

Henning Idsøe, Mohamed Hamid, Thomas Jordbru, Linga Reddy Cenkeramaddi and Baltasar Beferull-Lozano
Intelligent Signal Processing and Wireless Networks (WISENET) Lab.
Department of Information and Communication Technology
University of Agder, 4879, Grimstad, Norway

Abstract—In this paper, we experimentally validate the functionality of a developed algorithm for spectrum cartography using adaptive Gaussian radial basis functions (RBF). The RBF are strategically centered around representative centroid locations in a machine learning context. We assume no prior knowledge about neither the power spectral densities (PSD) of the transmitters nor their locations. Instead, the received signal power at each location is estimated as a linear combination of different RBFs. The weights of the RBFs, their Gaussian decaying parameters and locations are jointly optimized using expectation maximization with a least squares loss function and a quadratic regularizer. The performance of adaptive RBFs based spectrum cartography is shown through measurements using a universal software radio peripheral, a customized node and LabView framework. The obtained results verify the ability of adaptive RBF to construct spectrum maps with an acceptable performance measured by normalized mean square error (NMSE).

Keywords— Spectrum cartography, power spectrum maps, Adaptive radial basis functions, Experimental validation.

I. INTRODUCTION

Many wireless communications related applications including network planning, frequency reuse, coverage prediction, interference management, opportunistic spectrum access and cognitive radios require spatial radio spectrum awareness [1]–[4]. This spectrum awareness is achieved by building spatial, frequency and time dependent radio environment maps (REMs) under a framework called spectrum cartography. Throughout the rest of this paper, REMs and spectrum cartography will be used interchangeably to refer to received signal power maps. Spectrum cartography is a regression problem which is performed by collecting geo-localized measurements followed by spatial regression [5].

There are several techniques proposed for spectrum cartography including Kriging interpolation [5], [6], dictionary learning [7], sparsity aware regression [8], basis expansion [9], matrix completion [10] and reproducing kernel Hilbert space (RKHS) regression [11]–[13]. These techniques are briefly surveyed in [14]. To the best of the authors' knowledge, even though there exist diverse schemes for spectrum cartography, each of these schemes however has at least one of the following three limitations [14].

- 1) Some information regarding the transmitters' parameters and locations are needed.
- 2) Spatially dense measurements are required which is costly in terms of energy and communication bandwidth.
- 3) Basis functions are chosen statically with no adaptation based on the measurements.

In [14], the aforementioned limitations are overcome by developing a spectrum cartography algorithm that adapts the parameters of the basis functions based on a relatively lower density of measurements with no prior information about the transmitters. This goal is achieved by using RBF that are centered at strategic informative centroids locations instead of using kernels directly centered on sensors locations.

In view of the theoretical foundations of adaptive RBF based spectrum cartography provided in [14], this paper presents an experimental validation of the algorithm in two aspects. At first, the functionality of the algorithm is shown in real radio propagation environment. Secondly, in contrast to the simulations findings, measurements' performance is evaluated. Moreover, to the best of our knowledge, no experimental studies have been conducted regarding spectrum cartography prior to our campaign being reported in this paper. Therefore, the measurements setup and methodology is a stand alone contribution of this paper which can be used for implementing other spectrum cartography algorithms for comparison and bench marking purposes.

The remaining of this paper is structured as follows. Section II shows the system model. Section III presents the main contribution of [14] which is adaptive RBF with representative centroids based cartography. Measurements setup, results and findings are shown in Section IV. Finally, Section V concludes the paper.

Notation - Upper case bold letters are used to denote matrices such as $\mathbf{C} \in \mathbb{R}^{M \times N}$ while the element corresponding to the i^{th} row, j^{th} column of \mathbf{C} is denoted as $[C]_{ij}$. Column vectors are denoted by lower case bold letters as \mathbf{c} with c_i being the i^{th} entry of vector \mathbf{c} . For scalars, non-bold letters are used. \mathbf{C}^T and \mathbf{C}^{-1} are the transpose and inverse of matrix \mathbf{C} , respectively. The Identity matrix of size L is denoted by \mathbf{I}_L . $\mathbf{1}$ denotes an all one vector.

II. SYSTEM MODEL

The task of spectrum cartography is to construct a complete REM having a finite number of sensors. Consider an area $\mathcal{A} \subseteq \mathbb{R}^2$ that contains a set of N sensors that are aware of their locations. We define \mathcal{X} to be the set of the sensors locations where $\mathcal{X} \subset \mathcal{A} = \{\mathbf{x}_1, \mathbf{x}_2, \dots, \mathbf{x}_n\}, 1 \leq n \leq N$. Each sensor located at \mathbf{x}_i is providing a fusion center (FC) with a measurement of the received signal power $y_i(t)$ on its location at time t . Therefore, we define the measurements set at time t as $\mathcal{Y}(t) \in \mathbb{R} = \{y_1(t), y_2(t), \dots, y_n(t)\}, 1 \leq n \leq N$. The

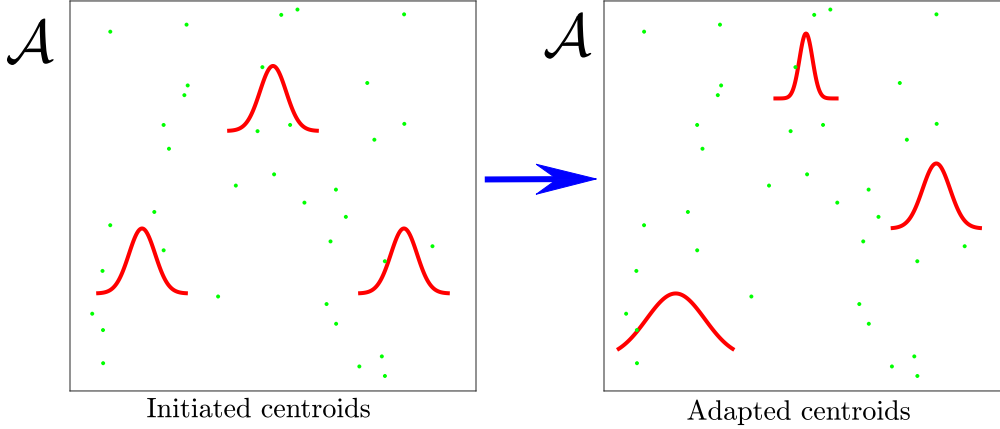


Fig. 1: Graphical illustration of adaptive RBF algorithm based spectrum cartography. The left sub-figure shows an arbitrary three initial centroids locations and their Gaussian decaying parameters as shown by the red curves while the green dots represent arbitrary sensors locations. The right sub-figure depicts the adapted RBF centroids and their Gaussian decaying parameters after convergence. All the curves and data in the figure are for illustrative purposes.

learning set that contains both the measurements and the sensors is denoted as $\mathcal{Z}(t) \in \mathbb{R}^3 = \{\mathbf{z}_1(t), \mathbf{z}_2(t), \dots, \mathbf{z}_N(t) | \mathbf{z}_i = (\mathbf{x}_i, y_i(t))\}$. Throughout the rest of this paper we consider instantaneous spectrum cartography with no learning along the time dimension, accordingly we omit the time dependency hereafter. The estimated cartography is denoted from here on as $\hat{h}(\mathbf{x}) : \mathbb{R}^3 \rightarrow \mathbb{R}$ while the actual cartography is denoted as $h(\mathbf{x})$. Cartography estimation is performed by the FC that receives all measurements.

The RBF based learning assumes that each point on the learning set, (\mathbf{x}_n, y_n) , affects the target function on any location \mathbf{x} as a function of the Euclidean distance between \mathbf{x} and \mathbf{x}_n . Considering REM as a function to be learned with the standard form of RBF, the learning REM is given by:

$$\hat{h}(\mathbf{x}) = w_0 + \sum_{i=1}^{N-1} w_i \exp(-\gamma_i \|\mathbf{x} - \mathbf{x}_i\|^2) \quad (1)$$

where w_0 is a constant offset that represent the background noise, w_1, \dots, w_{N-1} , are weighting parameters for the contribution of the different RBF, γ_i is a Gaussian decaying parameter for the i^{th} RBF. Applying (1) to the learning set would result in

$$\Phi \mathbf{w} = \mathbf{y} \quad (2)$$

where $\Phi = [\mathbf{1}_N | \tilde{\Phi}]$, $\tilde{\Phi} \in \mathbb{R}^{N \times N}$ with each element being $\tilde{\Phi}_{nk} = \exp(-\gamma_k \|\mathbf{x}_n - \mathbf{x}_k\|^2)$, $\mathbf{w} = [w_0, w_1, \dots, w_{N-1}]^T$ and $\mathbf{y} = [y_1, y_2, \dots, y_N]^T$

Accordingly, \mathbf{w} is found by

$$\mathbf{w} = \Phi^{-1} \mathbf{y} \quad (3)$$

The solution given by (3) implies finding N parameters from N observations which can be computationally expensive for large data sets. Moreover, Φ is not always invertible. To overcome these two limitations, representative centroids to locate the RBF is proposed as explained in the next section.

III. ADAPTIVE REPRESENTATIVE RBF

Now instead of centering the RBF around the sensor locations, K representative centroids are chosen for the RBF. The location of the centroids are denoted as μ_1, \dots, μ_K . Consequently, the cartography learning model represented by (1) is modified as:

$$\hat{h}(\mathbf{x}) = w_0 + \sum_{k=1}^K w_k \exp(-\gamma_k \|\mathbf{x} - \mu_k\|^2) \quad (4)$$

which is rewritable as

$$\Theta \mathbf{w} = \mathbf{y} \quad (5)$$

where $\Theta = [\mathbf{1} | \tilde{\Theta}]$, $\tilde{\Theta} \in \mathbb{R}^{N \times K}$ composed as $\tilde{\Theta}_{nk} = \exp(-\gamma_k \|\mathbf{x}_n - \mu_k\|^2)$, $1 \leq n \leq N, 1 \leq k \leq K$.

To estimate the cartography on \mathcal{A} , following model parameters need to be optimized jointly

- 1) The RBF centroids positions, μ_1, \dots, μ_K .
- 2) The weights vector \mathbf{w} .
- 3) The Gaussian decaying parameters $\gamma_1, \dots, \gamma_K$.

The joint optimization of these parameters, a least square solution is considered as

$$\min_{\mathbf{w}, \gamma_1, \dots, \gamma_K, \mu_1, \dots, \mu_K} \sum_{n=1}^N (y_n - \hat{h}(\mathbf{x}_n))^2 + \lambda \|\mathbf{w}\|^2 \quad (9)$$

where λ is a positive constant that trades off the estimator bias and variance [15]. Moreover, $\lambda > 0$ guarantees a solution to (9) even if $\Theta \Theta^T$ is a singular matrix (see (6)).

To solve the optimization problem (9) for \mathbf{w} , μ_1, \dots, μ_K , and $\gamma_1, \dots, \gamma_K$, we propose to use expectation maximization based optimization as in Algorithm 1.

For initializing the centroids locations μ_1, \dots, μ_K , either K -means clustering considering the sensors' locations or Cartesian grid over \mathcal{A} can be used. On the other hand, the Gaussian decaying parameters $\gamma_1, \dots, \gamma_K$ can all be assigned a same value for initialization. Fig. 1 illustrates graphically the idea of RBF adaptation exploiting Algorithm.

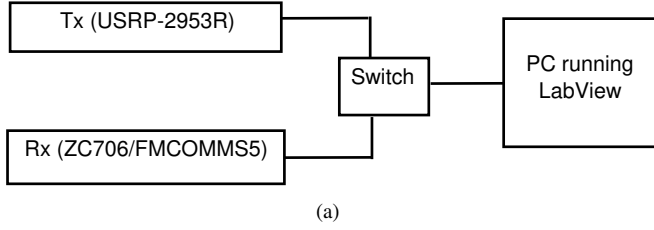


Fig. 2: (a) Measurement setup. (b) A picture of measurements location and setup

Data: Initialize the decaying parameters, $\gamma_1, \dots, \gamma_K$ and the centroids μ_1, \dots, μ_K ;

while *no convergence* **do**

Fix $\gamma_1, \dots, \gamma_K, \mu_1, \dots, \mu_K$ and solve for \mathbf{w} as

$$\mathbf{w} = (\Theta^T \Theta + \lambda \mathbf{I}_K)^{-1} \Theta^T \mathbf{y} \quad (6)$$

Fix $\mathbf{w}, \mu_1, \dots, \mu_K$ and solve for $\gamma_1, \dots, \gamma_K$, using gradient descent as

$$\gamma_k \leftarrow \gamma_k - \alpha \sum_{n=1}^N \left(y_n - \hat{h}(\mathbf{x}_n) \right) \cdot \|\mathbf{x}_n - \mu_k\|^2 \cdot \left(w_k \exp(-\gamma_k \|\mathbf{x}_n - \mu_k\|^2) \right) \quad (7)$$

¹ Fix $\mathbf{w}, \gamma_1, \dots, \gamma_K$ and solve for μ_1, \dots, μ_K , using gradient descent as

$$\mu_k \leftarrow \mu_k + 2\alpha \gamma_k \sum_{n=1}^N \left(y_n - \hat{h}(\mathbf{x}_n) \right) \cdot (\mathbf{x}_n - \mu_k) \cdot \left(w_k \exp(-\gamma_k \|\mathbf{x}_n - \mu_k\|^2) \right) \quad (8)$$

end

Algorithm 1: Adaptive RBF cartography

IV. MEASUREMENTS

This section presents the measurements setup and obtained results which is the contribution of this paper.

A. Measurements setup

The basic task of our measurements setup is to have the components of the adaptive RBF based cartography. These components are transmitters, sensors and a fusion center. For simplicity we adopted a setup consists of one transmitter, one sensor that moves and sense in different locations and a computer that controls both the transmitter and the sensor(s) and acts as a fusion center. Fig. 2(b) shows the adopted measurements setup with the equipment and parameters as in Table I. Fig. 2(b) shows a picture of the measurement location and setup

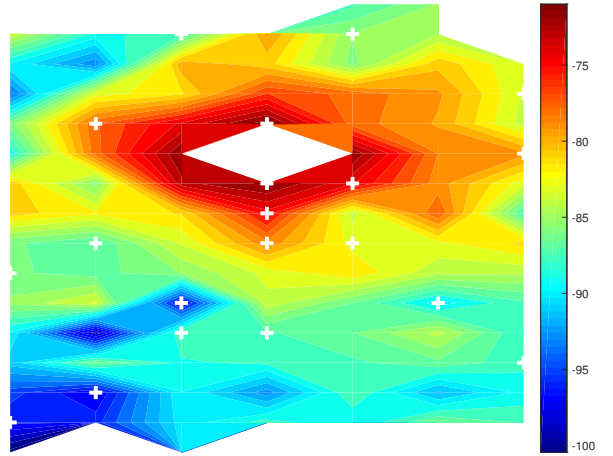


Fig. 3: Obtained spectrum map when using 50 measurements for learning and $K = 10$ centroids. The white crosses represent the measurements locations

Following are important remarks regarding the measurements setup:

- 1) ZC706 /FCOMM5S SDR which used as a sensor is a software defined radio (SDR) that is developed by the authors of this paper and and its performance is evaluated in [16].
- 2) The operating frequency of 5.41 GHz is chosen after scanning several other frequencies and that particular frequency is found vacant at the time and location of the measurements.
- 3) Binary phase shift keying (BPSK) is chosen arbitrarily as the main concern is to have a wireless transmission regardless of the modulation type and transmitted information.
- 4) A BPSK signal of a sample rate of 1.0 MS/S, would result in a main lobe bandwidth of 2.0 MHz. Therefore, a reception bandwidth of 3.0 MHz assures that the whole

TABLE I: Measurements Equipment and Parameters

Device/Parameter	Type/Value
Transmitter	NI-USRP 2953R
Sensor(s)	ZC706 /FCOMM5S 2953R SDR
Center frequency	5.41 GHz
Modulation	BPSK
Sample rate	1.0 MS/S
Reception bandwidth	3.0 MHz

TABLE II: Obtained NMSE for measurements and simulations, $N = 50$

Number of centroids	Measurements
5	-7.9 dB
10	-8.7 dB
20	-9.7 dB

energy contained in the main lobe will be received with extra energy contained in the first side lobe.

5) The switch is used to control both the transmission and sensing through the same PC.

The location of the measurements is a polyhedron room where a Cartesian grid of $0.5\text{m} \times 0.5\text{m}$ is made to determine the measurements locations set $\mathcal{X}_{mes} \subset \mathcal{A}$ as the crossings of this grid. The largest dimensions of the area within the room that is capable of hosting the measurements are 7.5m and 3.0m . Consequently, the measurements points set, \mathcal{X}_{mes} , are expressible as $\mathcal{X}_{mes} = \mathcal{U} \times \mathcal{V}$, $\mathcal{U} = \{0, 0.5, 1, \dots, 3\}$, $\mathcal{V} = \{0, 0.5, 1, \dots, 7.5\}$. The resultant measurements set consists of 112 points. However, 12 points are not feasible because they are either corners or there exist some unmovable furniture on them. Therefore, 100 measurements points are considered which is divided into a learning set, \mathcal{X}_{ler} , and a verification set, \mathcal{X}_{ver} each of them contains 50 points, learning set points are chosen uniformly randomly and the rest of measurements points are left for verification. Hence, $\mathcal{X}_{ler} \cap \mathcal{X}_{ver} = \emptyset$ and $\mathcal{X}_{ler} \cup \mathcal{X}_{ver} = \mathcal{X}_{mes}$.

For the quantitative evaluation, the normalized mean square error (NMSE) of the estimator using the measured values is used which is calculated as

$$\text{NMSE} = E \left[\frac{|h(\mathbf{x}) - \hat{h}(\mathbf{x})|^2}{|h(\mathbf{x})|^2} \right]$$

with $E[\cdot]$ denoting the expected value and $\mathbf{x} \in \mathcal{X}_{ver}$

B. Measurements results

Hereafter, the obtained results from the measurements are presented and analyzed.

Fig. 3 shows the reconstructed power spectrum map using $K = 10$ centroids followed by a quantitative analysis by means of obtained NMSE when changing the number of centroids as in Table II. As expected, the larger the number of centroids, the better the performance.

V. CONCLUSIONS

An experimental validation of adaptive radial basis functions based spectrum cartography algorithm is carried out.

The theoretical essence of the algorithm is to perform spatial interpolation for constructing power spectrum maps using strategically centered adaptive Gaussian radial basis functions. The centroids locations optimized jointly with the Gaussian decaying parameters and the linear model weights. The measurements findings validate the theory and show the influence of the number of centroids on the performance of the algorithm.

ACKNOWLEDGMENT

This work was supported by the FRIPRO TOPPFORSK grant 250910/F20 from the Research Council of Norway.

REFERENCES

- [1] A. Galindo-Serrano, B. Sayrac, S. B. Jemaa, J. Riihijärvi, and P. Mähönen, "Harvesting MDT data: Radio environment maps for coverage analysis in cellular networks," in *8th Int. Conf. Cognitive Radio Oriented Wireless Networks*, Jul 2013, pp. 37–42.
- [2] S. Grimoud, S. B. Jemaa, B. Sayrac, and E. Moulines, "A REM enabled soft frequency reuse scheme," in *IEEE Global Commun. Conf.*, Dec 2010, pp. 819–823.
- [3] J. D. Naranjo, A. Ravanshid, I. Viering, R. Halfmann, and G. Bauch, "Interference map estimation using spatial interpolation of MDT reports in cognitive radio networks," in *IEEE Wireless Commun. and Networking Conf.*, Apr 2014, pp. 1496–1501.
- [4] S. Debroy, S. Bhattacharjee, and M. Chatterjee, "Spectrum map and its application in resource management in cognitive radio networks," *IEEE Trans. Cognitive Commun. and Networking*, vol. 1, no. 4, pp. 406–419, Dec 2015.
- [5] A. B. H. Alaya-Feki, S. B. Jemaa, B. Sayrac, P. Houze, and E. Moulines, "Informed spectrum usage in cognitive radio networks: Interference cartography," in *IEEE 19th Int. Symp. Personal, Indoor and Mobile Radio Commun.*, Sep 2008, pp. 1–5.
- [6] G. Bocolini, G. Hernández-Peñaloza, and B. Beferull-Lozano, "Wireless sensor network for spectrum cartography based on kriging interpolation," in *IEEE 23rd Int. Symp. Personal, Indoor and Mobile Radio Commun.*, Sep 2012, pp. 1565–1570.
- [7] S. J. Kim and G. B. Giannakis, "Cognitive radio spectrum prediction using dictionary learning," in *IEEE Global Commun. Conf.*, Dec 2013, pp. 3206–3211.
- [8] J. A. Bazerque and G. B. Giannakis, "Distributed spectrum sensing for cognitive radio networks by exploiting sparsity," *IEEE Trans. Signal Process.*, vol. 58, no. 3, pp. 1847–1862, Mar 2010.
- [9] J. A. Bazerque, G. Mateos, and G. B. Giannakis, "Group-lasso on splines for spectrum cartography," *IEEE Trans. Signal Process.*, vol. 59, no. 10, pp. 4648–4663, Oct 2011.
- [10] G. Ding, J. Wang, Q. Wu, Y. D. Yao, F. Song, and T. A. Tsiftsis, "Cellular-base-station-assisted device-to-device communications in TV white space," *IEEE J. Sel. Areas Commun.*, vol. 34, no. 1, pp. 107–121, Jan 2016.
- [11] D. Romero, S. J. Kim, and G. B. Giannakis, "Online spectrum cartography via quantized measurements," in *49th Ann. Conf. Inform. Sci. and Syst.*, Mar 2015, pp. 1–4.
- [12] D. Romero, S. J. Kim, López-Valcarce, and G. B. Giannakis, "Spectrum cartography using quantized observations," in *IEEE Int. Conf. Acoust., Speech and Signal Process.*, Apr 2015, pp. 3252–3256.
- [13] D. Romero, S. Kim, G. B. Giannakis, and R. López-Valcarce, "Learning power spectrum maps from quantized power measurements," *CoRR*, vol. abs/1606.02679, 2016. [Online]. Available: <http://arxiv.org/abs/1606.02679>
- [14] M. Hamid and B. Beferull-Lozano, "Non-parametric spectrum cartography using adaptive radial basis functions," in *42nd IEEE Int. Conf. Acoustics, Speech and Signal Processing*, Mar. 2017, pp. 3599–3603.
- [15] R. W. K. Arthur E. Hoerl, "Ridge regression: Applications to nonorthogonal problems," *Technometrics*, vol. 12, no. 1, pp. 69–82, 1970.
- [16] T. Jordbru, H. Idsøe, L. R. Cenkeramaddi, B. Beferull-Lozano, and M. Hamid, "Radio measurements on a customised software defined radio module: A case study of energy detection spectrum sensing," in *IEEE Int. Instrumentation and Measurement Technology Conf.*, May. 2017, pp. –.